MANY-PARTICLE EQUILIBRIUM PROPERTIES OF GLASSY CHALCOGENIDES: NUMERICAL SIMULATIONS IN THE COULOMB GLASS MODEL

M. CARAVACA[*], F. GIMENO, A. SOTO-MECA
University Centre of Defence at the Spanish Air Force Academy, Coronel Lopez Peña st., n/n, 30720 Santiago de la Ribera, Murcia, Spain

In this paper, we investigate some many-particle equilibrium properties of the Coulomb glass model to deepen into the thermal behavior of glassy chalcogenides. Concretely, we focus on the dependence of the energy on the temperature, the many-particle density of states and the absorbed and emitted power. The results show an interesting conclusion: at very low temperatures, the effect of soft transitions, called soft dipoles, is dominant, which gives the material its characteristic glassy behavior, characterized by slow dynamical rates.

1. Introduction

In some recent publications, the connection between glassy chalcogenides and Coulomb glasses has been clearly pointed out [1-4]. Coulomb (or equivalently, electron) glasses are systems with localized electronic states due to the presence of disorder and long-range interactions between carriers. When the temperature is low enough, and the disorder and interaction typical energies become relevant, the system shows glassy behavior [5].

The study of the equilibrium properties of Coulomb glasses can be employed to deepen into the nature of the glassy state of amorphous chalcogenides. In a previous work, some of the authors introduced the extension of the one-particle equilibrium properties, namely, the minimum of the one-particle density of states (DOS) and the fluctuation-dissipation theorem (FDT), to characterize some key aspects out of equilibrium [3]. However, another kind of equilibrium properties, the many-particle ones, deserves a separate study in order to achieve a deep comprehension of the glassy dynamics of these systems. Among them, in this work, we will focus on the total energy of the system, the many-particle density of states (MPDOS) and the total emitted and absorbed power, to show that the intrinsic dynamics of the Coulomb glass is dominated by electronic transitions that constantly occur back and forth, called *soft dipoles*.

The standard tight-binding Hamiltonian that describes the Coulomb glass model is [6]

$$H = \sum_i \phi_i n_i + \sum_{i<j} \frac{(n_i - K)(n_j - K)}{r_{ij}} \tag{1}$$

As described in previous works [4-6], ϕ_i is the so-called *random site potential*, which represents the structural disorder of the sample, n_i is the occupancy number of site i, which can either be 0 or 1, K is the compensation, which ensures the electrical neutrality of the system, and r_{ij} is the distance between sites i and j.

The total potential of each site is called the *site energy*, defined as follows

---

* Corresponding autor: manuel.caravaca.upct@hotmail.es

$$\epsilon_i = \phi_i + \sum_{j \neq i} \frac{(n_j - K)}{r_{ij}} \tag{2}$$

Coulomb glasses behave like doped insulating systems, in which the transitions are performed by electrons jumping from a occupied to an empty site, which positions match with that of the impurities of the system, due to the strong localization of electronic states [5, 6]. Accomplishing one of these particular transitions is equivalent to change from a particular electronic configuration labeled as α to another one β, differentiated by the occupancy of one site. The energy difference between α and β is, due to Eq. (1)

$$\Delta E_{\alpha\beta} = \sum_i \phi_i \left(n_i^\beta - n_i^\alpha \right) + \sum_{i<j} \sum_{j \neq i} \frac{\left(n_i^\beta - K \right)\left(n_j^\beta - K \right) - (n_i^\alpha - K)(n_j^\alpha - K)}{r_{ij}} \tag{2}$$

where n_i^α and n_i^β are components of the occupancy vector before and after the transition, respectively. If we consider an individual jump of an electron, between generic sites l and k, the occupancy vectors only differ in these subscripts, and then Eq. (2) reduces to

$$\Delta E_{\alpha\beta} = \Delta E_{kl} = \epsilon_l - \epsilon_k - \frac{1}{r_{kl}} \tag{3}$$

This energy difference can be interpreted as the difference of site energies minus an *excitonic* term, which is the Coulomb interaction of the pair electron-hole created, responsible of the appearance of the Coulomb gap in the DOS [5]. The key aspect of Eq. (3) is that, from the ground state, the system has to be stable to one-particle transitions, $\Delta E_{kl} \geq 0$, so the distance between the occupied and the empty site is restricted by the expression

$$r_{kl} > \frac{1}{\epsilon_l - \epsilon_k} \tag{4}$$

From this last equation we infer that, as we approach the ground state, the electrons have to jump increasingly long distances, because the difference of site energies approaches zero.

A soft dipole is a special kind of transition, constituted by sites with great differences of site energies, but very near in distance, in such a way that the excitonic term in Eq. (3) compensates the energy difference. These transitions are repeated back and forth and are very time consuming. Coulomb glasses present a distribution of local energy minima, called the *pseudo ground states* and, at very low temperatures. Generally, the system gets stacked in one of them for a long time, mainly due to the dynamic of soft dipoles, thus taking a great transition time to move to another minimum of lower energy [5].

2. Mathematical model and numerical details

We study the equilibrium properties of semiconductor samples doped with impurities randomly placed, in the regime of strong localization and very low temperatures. This fact is equivalent to assume that the system behaves as a dielectric material and transitions happen by electrons jumping between impurities, in the regime of variable range hopping [6,7]. We consider that the position of the electron matches that of the impurity, since the value of the localization length, ξ, is considered very small [5]. We study squared samples of lateral dimension L and implement periodic boundary conditions.

The units employed in the numerical simulations are: $1/l_0$ is the energy and temperature unit, $l_0 = L/\sqrt{N}$ is the length unit, once taken the electron charge, e, and Boltzmann constant, k_B, as the unit. In the present simulations we consider a range of temperatures $T \in [0.001, 0.3]$. We

consider systems sizes ranging between 500 and 2000 sites, setting a minimum distance between them of 0.2. The range of disorder is $W = 2$ and the localization length is $\xi = 1$. Our time unit is the characteristic electron-phonon time, τ_0. To ensure the neutrality of the system we choose $K = 1/2$, and consider that each particle only interacts with its nearest image. In that way, we do not perform Ewald summation.

We employ two kinds of algorithms in our simulations. For the lowest temperatures we use optimization algorithms [8, 9], specifically designed to get the lowest energy configurations of the system. The results obtained allow us to apply the standards of statistical mechanics in order to calculate magnitudes in equilibrium. These algorithms fail at higher values of T so, in those cases, we employ another kind of method. We perform Monte Carlo simulations by means of the Tsigankov *et al.* hybrid algorithm [10], at high enough temperatures, so the system quickly reaches thermal equilibrium. At very low T this last method becomes inefficient because the system does not reach the equilibrium state easily. The employment of both algorithms simultaneously allows us to study a wider range of temperatures.

For simulations using the lowest energy configurations, a statistical average has been carried out over 1000 samples, *i. e.*, different arrangements of sites. For the Monte Carlo algorithm, the total number of simulations, n_{tot}, is defined as $n_{\text{tot}} = n_{\text{s}} \cdot n_{\text{occ}}$, where n_{s} is the number of samples and n_{occ} is the number of initial occupations of electrons per sample. In this work, we have set $n_{\text{s}} = 100$ and n_{occ} ranging between 10 and 50.

3. Results and discussion

Energy as a function of temperature

Now we go on analyzing the many-particle equilibrium properties of Coulomb glasses. We start by studying the dependence of the total energy of the system on the temperature. First of all, let us suppose a non-interacting system. We can write the average energy per particle of the system, $\langle E \rangle / N$, as follows

$$\frac{\langle E \rangle}{N} = \int_{-\infty}^{\infty} \epsilon \, g(\epsilon) \mathrm{d}\epsilon = g_0 \int_{-\infty}^{\infty} \epsilon \, f(\epsilon) \mathrm{d}\epsilon \tag{5}$$

Here $g(\epsilon)$ is the DOS of a single particle. This function presents no singularity in absence of interactions and, at very low temperatures, is a good approximation to assume it is constant [11]. Therefore, it has been taken out of the integral in Eq. (5). We call that constant value g_0, and the probability of site occupancy, $f(\epsilon)$. In equilibrium, this last function corresponds to a Fermi-Dirac distribution (FDD, herein) at the room temperature, T [6].

We can develop an intuitive argument to evaluate the dependence of $\langle E \rangle$ on temperature. To do this, we rely on the particular form of the functions $g(\epsilon)$ and $f(\epsilon)$, shown qualitatively in Figure 1. We assume that the site energy ϵ is fixed with respect to the ground level.
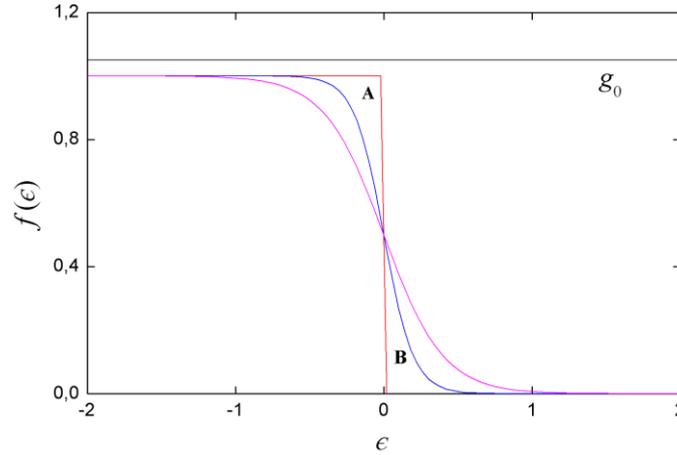
Fig. 1. Qualitative form of the probability of occupancy, $f(\epsilon)$, and the density of states, g_0, for a disordered system with strong localization in the absence of interactions, for several temperatures (colored lines). The value of g_0 is independent of T.

At any temperature, the DOS has a constant value, while the FDD depends on T. At $T = 0$, it is a descending step function centered on the Fermi level (red line), while at $T \neq 0$ the slope of the function in the central section begins to increase (other colours). By employing the theoretical expression of the FDD [12] we can easily find that the slope in this section is equal to $1/T$. If we look at the area near the Fermi level in Figure 1, we notice that the electrons that were in the region A at $T = 0$ have "moved" to the region B once the temperature has increased. The typical horizontal displacement is of the order of T, since the vertical height of the FDD is constant. Furthermore, the number of displaced electrons is proportional to the area of the region A. We approximate that region by a right triangle of hypotenuse $1/T$, which is the slope of the FDD. The area of the triangle is T. The multiplication of the number of electrons that have moved on average by the typical shift in energy gives the T dependency of the total energy. Thus

$$\langle E \rangle \propto T^2$$

We can calculate in a more rigorous way the integral given in Eq. (5). If we write the expression of $f(\epsilon)$ and we perform the change of variable $x = \epsilon/k_{\mathrm{B}}T$, we obtain

$$\frac{\langle E \rangle}{N} = g_0 (k_{\mathrm{B}}T)^2 \int_{-\infty}^{\infty} \frac{x}{1 + \exp(x)}\, \mathrm{d}x$$

If we calculate the value of $\langle E \rangle$ relative to the energy of the ground level, $\langle E_0 \rangle$, and consider the form of $f(\epsilon)$ when $T = 0$, we can modify the previous expression as follows

$$\frac{\langle E \rangle - \langle E_0 \rangle}{N} = g_0 (k_{\mathrm{B}}T)^2 \int_{-\infty}^{0} x \left(\frac{1}{1 + \exp(x)} - 1 \right) \mathrm{d}x + \int_{0}^{\infty} \frac{x}{1 + \exp(x)}\, \mathrm{d}x =$$

$$= 2 g_0 (k_{\mathrm{B}}T)^2 \int_{0}^{\infty} \frac{x}{1 + \exp(x)}\, \mathrm{d}x = \frac{\pi^2}{6} g_0 (k_{\mathrm{B}}T)^2 \tag{6}$$

confirming the quadratic dependence of the energy on the temperature. This calculation is independent of the degree of localization of the system.

Now, we try to extend the analysis above to the interacting case, whose result now depends on the degree of localization. We will focus on the strong localized regime. When the interaction among the particles in the system is not negligible, the approximation of considering

the density of states as a constant, with a value independent of the temperature, fails. In this case, $f(\epsilon)$ is described again by a FDD at the room temperature [5]. The qualitative graphical representation of both $g(\epsilon)$ and $f(\epsilon)$ in this situation is shown in Figure 2. Again, ϵ is fixed with respect to the ground level. The solid line in the plot refers to the FDD, and the dashed line represents $g(\epsilon)$, which shows the characteristic form of the Coulomb gap.
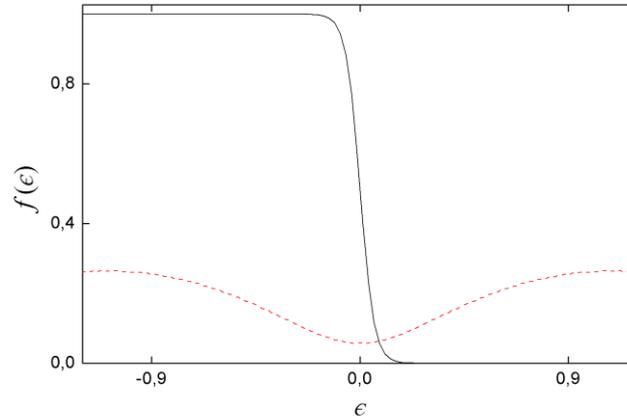

Fig. 2. Qualitative form of the probability of occupancy $f(\epsilon)$ (solid line) and the density of states $g(\epsilon)$ (dashed line) for a disordered interacting system with strong localization.The minimum of the density of states, g_0, depends on T and is approximately constant in the range of variation of $f(\epsilon)$.

At very low temperatures, the range of variation of $f(\epsilon)$ is very small, so the portion of density of states that lies in that range is almost constant. Again, we call that value g_0, considering that now it depends on the temperature. In a previous work, some of the authors determined that there is a direct linear dependency between g_0 and T for two-dimensional systems [3]. From this result and, by using the same argument that in the non-interacting case, we obtain that the dependence of the average energy on T is, in principle, of cubic order

$$\langle E \rangle \propto T^3 \tag{7}$$

due to the extra dependency on T introduced by g_0.

In this deduction we considered that transitions only occur in the inner zone of the gap. However, there are many other transitions that constantly occur back and forth, consisting of pairs whose difference between site energies is large [5]. These pairs are placed at very close distances so, as we argued before, the excitonic term (electron-hole) of the form $1/r$ in Eq. (3) compensates the energy difference, where r is the separation distance of the pair. These configurations are called weak transitions or soft dipoles [5,6].

We can calculate the contribution to the total energy of the system due to these soft transitions as a function of T. Firstly, let us suppose a system with only two sites, one occupied and one empty. We have two possible configurations, labeled with energies ϵ_1 and ϵ_2. Do not confuse the nomenclature we use to designate the site energies of the system. If we set to zero the energy of the ground level, we can rewrite them as 0 and ϵ, respectively. If we suppose that the system is in equilibrium, the average energy is

$$\langle E \rangle = \frac{\epsilon \exp(-\epsilon/k_B T)}{1 + \exp(-\epsilon/k_B T)} = \epsilon f_d(\epsilon)$$

Function $f_d(\epsilon)$ is again a FDD at T. In this expression, and in the following ones, subscript "d" in the magnitudes refers to dipoles. In a many-particle system, dipole-dipole interaction is much smaller than the interaction between particle pairs [5], so it is a good approximation to

consider soft dipoles as isolated entities. Therefore, the contribution to the total energy of the system, with respect to the fundamental level, due to these soft dipoles can be written as

$$\frac{\langle E_{\mathrm{d}} \rangle - E_0}{N} = \int_{-\infty}^{\infty} \epsilon g_{\mathrm{d}}(\epsilon) f_{\mathrm{d}}(\epsilon) \mathrm{d}\epsilon$$

In this expression, $g_{\mathrm{d}}(\epsilon)$ is the density of free dipoles per volume unit. As in the deduction for the non-interacting case, we may consider $g_{\mathrm{d}}(\epsilon)$ as a constant in the range of low temperatures, due to the isolation approximation (no interaction between dipoles). As a result, and by virtue of Eq. (6)

$$\langle E_{\mathrm{d}} \rangle \propto T^2$$

Under the considered approximations, the dependence of the total energy on T is dominantly of quadratic order in the range of very low temperatures.

The data obtained from our simulations are consistent with this result, and reveal the importance of the soft dipoles at very low temperatures. The calculation of the equilibrium energy, with respect to the ground level, for very low values of T, is carried out using the lowest energy levels of the system

$$\langle E \rangle - \langle E_0 \rangle = \frac{1}{Z} \sum_{i=1}^{n_{\mathrm{n}}} (E_i - E_0) \exp\left[-\frac{(E_i - E_0)}{k_{\mathrm{B}} T} \right] \qquad (8)$$

The sum extends to n_{n}, the maximum number of low energy levels calculated, using a specific configuration algorithm, such as that described in [8,9]. E_i is the energy of each level, E_0 is the energy of the ground level and Z is the canonical partition function. The results obtained from our simulations are shown in Figure 3. The average energy per particle in equilibrium respect to the ground level is represented against T, using a double logarithmic scale. The data has been obtained for systems of sizes 500 (black squares) and 1000 (red dots), with a number of samples in the order of 1000, for each temperature. The maximum number of levels, n_{n}, is in the order of 10000. Data errors are determined by the standard deviation of the energy of the samples, and are in the order of the spot size. Temperature ranges between 0.001 and 0.011. From the figure, it is depicted that the values of the energies in equilibrium are practically independent of size. From the linear fit of the data corresponding to $N = 1000$ we obtain a slope of 2.06 ± 0.04, a fact that verifies the quadratic dependence of the energy at very low temperatures.
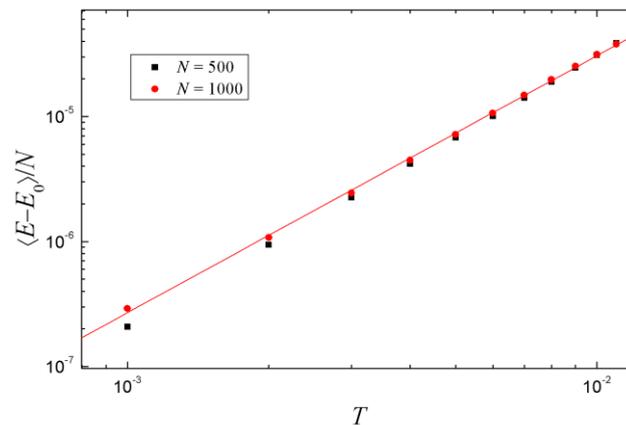

Fig. 3. Total energy per particle with respect to the ground level versus T, in a double logarithmic scale. The results are presented for samples of size 500 (black squares) and 1000 (red dots). The linear fit of the data for N = 1000 gives a value of 2.06 ± 0.04 for the slope of the line within the considered range of temperatures.

However, our simulations using the lowest energy configurations cannot cover a wide range of temperatures. As the sample size increases, the number of energy levels grows exponentially. Similarly, this number increases exponentially as a function of energy [5,6]. The discrete sum in Eq. (8) converges to the real infinite sum only at very low temperatures, where the Boltzmann function is narrower and the first energy levels dominate. The criterion chosen to determine the maximum temperature for this numerical problem is to consider that the Boltzmann factor of the last valid energy configuration, $\exp\left[-\left(E_{n_{\mathrm{n}}} - E_0\right)/k_{\mathrm{B}}T\right]$, is less than a certain very small value. Qualitatively, we choose as a limit that the argument of the exponential has a value -10, making the Boltzmann factor to be 0.0025. Thus the maximum temperature is $T_{\mathrm{max}} = \left(E_{n_{\mathrm{n}}} - E_0\right)/10$. For a typical system of size 1000 with 10000 low energy levels calculated, we obtain $E_{n_{\mathrm{n}}} - E_0 = 0.08$ and, thus, $T_{\mathrm{max}} = 0.013$. One way to test the usefulness of this approach is to reduce the number of maximum levels n_{n} in half and redo the calculation of the total energy of equilibrium. In our case, the divergence begins to be observed from a temperature $T = 0.012$, so the cut-off criterion selected in the exponential function is acceptable.

Nevertheless, it is possible to complete the curve $(\langle E \rangle - \langle E_0 \rangle)/N$ versus T for higher temperatures using Monte Carlo simulations. For this purpose we employ Tsigankov's *et al.* algorithm [10]. If T is high enough the system will quickly reach the equilibrium. In Figure 4 we represent together the values of the equilibrium energy per particle versus T, relative to the ground level, for both methods (adding data of Figure 3). A logarithmic scale was used on both axes. Data for sizes 500 (circles) and 1000 (triangles) are shown in the same plot. The open symbols correspond to simulations made by using the lowest energy configurations, this time employing 100000 calculated levels. The filled symbols represent the data obtained by Monte Carlo simulations. Errors of this final data set are determined from the standard deviation of the average equilibrium energy of each sample. We checked that this error is larger than the fluctuation associated to the equilibrium energy of each individual sample, so it can be considered as dominant. Still, it is the order of the size of the plotted point.

As shown in Figure 4, data obtained by means of the two methods collapse into a single curve for the whole temperature range under consideration. Thereby, a unique linear fit for all points is feasible. As we increase T, the cubic dependence of the energy starts to gain significance, as presented in Eq. (7), which only took into account the internal transitions in the gap. A linear fit for the whole range of temperature of the type

$$\frac{\langle E \rangle - E_0}{N} = \alpha T^2 + \beta T^3 \tag{9}$$

is performed.

From our data we obtain $\alpha = 0.31 \pm 0.05$ and $\beta = 1.30 \pm 0.04$. However, the data fit better to a dependence of the type

$$\frac{\langle E \rangle - E_0}{N} = \gamma T^\delta \tag{10}$$

From the fit, a value of $\delta = 2.3 \pm 0.2$ is obtained. The contrast between both expressions was performed by comparing the value of the reduced chi-squared value, χ^2, since both cases have the same degrees of freedom. The value of this coefficient is lower for the fit corresponding to Eq. (10) than for Eq. (9). For this reason, the first one is shown in Figure 4 (solid line) in spite of not having found a theoretical justification of it.
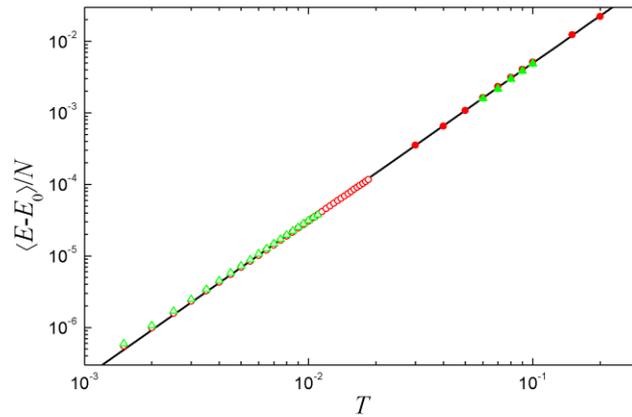
Fig. 4. Energy per particle relative to the ground level versus T, in double logarithmic scale. The calculated sizes are N = 500 (circles) y 1000 (triangles). The open symbols represent the data obtained from simulations using the lowest energy configurations. Solid symbols, those obtained by means of equilibrium Monte Carlo simulations. The straight line represents the fit given by Eq. (10).

Many-particle density of states

Another method to verify the dependence of the equilibrium energy on temperature requires the analysis of MDOS, which we call $G(E)$. We will suppose that E is the total energy of the system relative to the ground level. We can define the magnitude $G(E)\Delta E$ as the number of states per area unit whose total energy lie in the range $[E, E + \Delta E]$.

By using the lowest energy configurations found we can simply determine the form of $G(E)$ by making a histogram with the energies of these states. The representation of the histogram is shown in Figure 5 for a system of size 2000. The presence of the solid line will be justified below. This plot suggests an exponential dependence for the data. In fact, it can be determined that the dependence of $G(E)$ with the total energy of the system presents the shape of a stretched exponential

$$G(E) = k \exp(cE^\gamma) \tag{11}$$

where the exponent γ takes a value less than 1. Parameters k and c are both constant. To verify this dependence, let us return to Figure 5. The main objetive is to determine the value of γ. We extract data pairs from the histogram having as abscissa the central energy value of each box and as ordinate its corresponding height in the histogram. We will name $\tilde{G}(E)$ to the magnitude corresponding to the ordinate. The dependence of this new variable with E is the same as that of the function $G(E)$ given by the Eq. (11), so we can determine γ from the analysis of $\tilde{G}(E)$. If we carry out the fit of the above expression to the data pairs $E, \tilde{G}(E)$ we obtain a value $\gamma = 0.53 \pm 0.03$. The theoretical line given by the exponential fit is represented over the histogram in Figure 5.

In order to estimate the error of γ we have assumed that the histogram data correspond to a Poisson distribution. The error in each box is thus $\sqrt{n}$, where n is the number of event per box. The value of the exponent γ will be employed to give an alternative expression of the dependence of the average energy of the system on T, as discussed below.
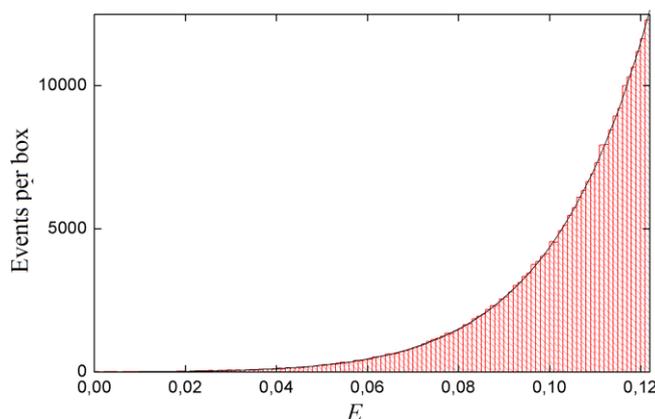
Fig. 5. Number of system states histogram in terms of the total energy versus the ground level, for a system of size 2000. The width of each box is .001. The solid line represents the fit of the expression given by Eq. (8) to the data extracted from the histogram.

We can develop an alternative calculation of the average energy of the system by employing the information given by the MDOS. If we use equilibrium statistical properties, the average total energy of the system is

$$\langle E \rangle = \frac{\int_{-\infty}^{\infty} EG(E)\exp\left(-\frac{E}{k_{\mathrm{B}}T}\right)\mathrm{d}E}{\int_{-\infty}^{\infty} G(E)\exp\left(-\frac{E}{k_{\mathrm{B}}T}\right)\mathrm{d}E} \tag{12}$$

with $G(E)$ given by Eq. (11). Again, we call E to the difference between the total energy of the system and the ground level. At low temperatures, and when the system is large enough, the product of multiplying functions $G(E)$ and $\exp(-E/k_{\mathrm{B}}T)$ is a narrow enough function to consider only its maximum as relevant [5,6]. To obtain this maximum value, we derive the integrand of Eq. (12), $\exp(E^{\gamma} - \beta E)$, where we have performed the change $\beta = 1/k_{\mathrm{B}}T$

$$\gamma E^{\gamma-1} - \beta = 0 \rightarrow E = \left(\frac{\beta}{\gamma}\right)^{\frac{1}{\gamma-1}}$$

From this result we obtain that the dependence of the average total energy on temperature has the form

$$\langle E \rangle \propto T^{\frac{1}{\gamma-1}}$$

From the fit we obtain the value $\gamma = 0.53 \pm 0.03$, so the total energy follows the expression

$$\langle E \rangle \propto T^{2.13 \pm 0.14}$$

This result is consistent with that obtained from Eq. (10), which strengthens the calculus of the dependence of the total energy of the system on T.

Absorbed and emitted power
In equilibrium, the total power absorbed by the system at a given temperature is equal to the total emitted power.

The former one is associated with the electronic transitions that increase the total energy of the system, yielded by the phonons at temperature T. By virtue of the electron-phonon

interaction, a phonon is destroyed in this process. The latter one has to do with transitions that reduce the total energy, resulting in the creation of a new phonon. The equality of these quantities in equilibrium is evident from our simulations. Again, we have used the configuration and Monte Carlo algorithms together to cover a wide range of temperatures.

Regarding the configuration algorithm, that employs the lowest energy configurations, first we evaluate every transition probability per time unit between calculated configurations. We consider only the transitions that increase energy, so we use the standard expression for the transition rate $\Gamma_{\alpha\beta}$ between two configurations in Coulomb glasses [5,6]

$$\Gamma_{\alpha\beta} = \tau_0^{-1} \exp\left(\frac{-2r_{ij}}{\xi}\right) \exp\left(\frac{-\Delta E_{\alpha\beta}}{k_B T}\right)$$

The treatment for transitions that reduce the energy is similar. The absorbed power is thus calculated as [5]

$$P(T) = \sum_{\alpha,\beta} \frac{\exp\left[-\frac{E_\alpha}{k_B T}\right]}{Z} \exp\left[-2r_{\alpha,\beta} - \frac{(E_\beta - E_\alpha)}{k_B T}\right] (E_\beta - E_\alpha)$$

In this expression, the first exponential term is the probability of finding the system in configuration α, while the second is the transition probability per time unit between the configurations α and β. The sum extends over each pair of configurations whose transition increases the energy. For the calculation, a number of samples of the order of 1000 has been used at each temperature. The error in the data is determined from the standard deviation of the considered samples.

For the Monte Carlo algorithm, we calculate the increasing and decreasing averaged total energy of the system separately, as a function of time. At equilibrium, the representation of these two quantities corresponds to a straight line. The slope of the plots has units of energy per time unit, and represents the value of the absorbed and emitted power, respectively, at each temperature. The error in the data is calculated again from the standard deviation associated with the samples.

Figure 6 shows in the same plot the data obtained by both methods. We represent only the absorbed power per particle P, dependent on temperature, in a double logarithmic scale, for sizes 500 (circles), 1000 (triangles) and 2000 (squares). The open symbols are related to the data obtained by the configuration algorithm and, the solid ones, by the Monte Carlo algorithm.

For convenience, we have added the representation of the energy as a function of temperature that was presented in Figure 4. The good linear behavior of the data suggests a dependence of the type

$$P \propto T^\lambda$$

From the slope of the line associated with the curve of the absorbed power we determine a value of $\lambda = 2.15$. This exponent is very similar to that obtained for the dependence of the total energy on temperature, through Eq. (10). The similarity between these two slopes is difficult to explain in a clear way. However, one can assume that, as in the case of energy, the largest contribution to the absorbed and emitted power comes from the soft dipoles. In our numerical calculations we have found that over 80% of the value of the power comes from these soft dipoles, regardless of temperature. To determine this percentage, we analyzed the total increasing and decreasing energies of the system, and compared these values with the same energies restricted only to the soft transitions. The chosen criterion for determining whether a pair of configurations forms a soft dipole involves selecting a cutoff in distances. Operationally, we choose that the distance between sites involving the soft transition, r_{ij}, is less than 1. In our systems, the maximum difference in site energies is of the order of 0.1, thus the excitonic factor $1/r_{ij}$

compensates the difference in one order of magnitude by virtue of Eq. (3). The criterion is enough to include the majority of the dipoles in the calculation.
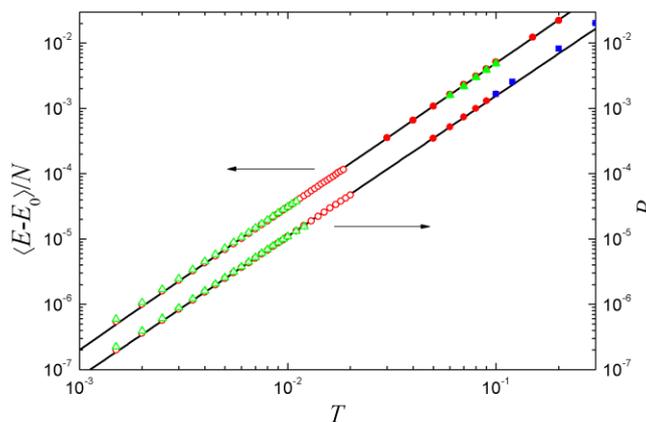

Fig. 6. Absorbed power per particle versus T, in double logarithmic scale. The calculated sizes are N = 500 (circles), 1000 (triangles) y 2000 (squares). The open symbols represent data obtained from simulations with the lowest energy configurations. The filled symbols are data obtained by equilibrium Monte Carlo simulations. The straight line represents the linear fit of the data. The graphical representation of Fig. 4 has been added.

4. Conclussions

In the present article we complete the numerical study of the one-particle equilibrium properties of glassy chalcogenides previously presented by some of the authors, this time focusing on the analysis of the many-particle properties. Concretely, the work is devoted to the study of the total energy of the system, the many-particle density of states and the absorbed and emitted power. To perform the numerical simulations, we employed a double algorithm approach in order to cover a wide range of temperatures. Apart of giving theoretical expressions for the dependence of the magnitudes on the temperature, we revealed an important information regarding the intrinsic dynamics of the Coulomb glass model at very low temperatures: the effects of the soft dipoles are dominant. The dynamical part of the study allowed us to state, by following the equilibrium dynamics of the energy and the power, that the forth and back transitions which characterize the soft dipoles dominate the total energy value at very low temperatures, and also provide over the 80% of the emitted and absorbed power of the system. This key fact becomes essential to understand the complicated dynamics of Coulomb glasses. Due to this fact, some of the authors are currently working on developing clustering numerical algorithms to treat the soft dipoles as a set of internal configurations. In such a way, it is possible to statistically estimate the effective time that the system spends in each particular set, and consider it as a black box.

References

[1] S. A. El-Hakim, M. A. Morsy, Radiat. Eff. Defect **169**, 313 (2014).
[2] M. Caravaca, J. Abad, Chalcogenide Lett. **11** (6), 287 (2014).
[3] M. Caravaca, F. Gimeno, J. L. Meseguer-Valdenebro, Chalcogenide Lett. **12** (5), 227 (2015).
[4] M. Caravaca, F. Gimeno, A. Soto-Meca, Chalcogenide Lett. **12** (8), 429 (2015).
[5] M. Caravaca, Conductividad y relajación en vidrios de Coulomb, PhD Thesis, Universidad de Murcia (2010).
[6] M. Pollak, M. Ortuño, A. Frydman, The Electron Glass, Cambridge University Press, Cambridge (2013).
[7] A. M. Somoza, M. Ortuño, M. Caravaca, M. Pollak, Phys. Rev. Lett. 101, 056601 (2008).
[8] A. Diaz-Sanchez, A. Möbius, M. Ortuño, A. Perez-Garrido, M. Schreiber, Phys. Stat. Sol. B

205 (1), 17 (1998).

[9] A. Diaz-Sanchez, M. Ortuño, M. Pollak, A. Perez-Garrido, A. Möbius, Phys. Rev. B **59** (2), 910 (1999).

[10] D. N. Tsigankov, E. Pazy, B. D. Laikhtman, A. L. Efros, Phys. Rev. B, **68** (13), 184205 (2003).

[11] B. I. Shklovskii, A. L. Efros, Electronic properties of doped semiconductors, Springer-Verlag, Berlin Heidelberg (1984).

[12] D. Chandler, An introduction to modern statistical physics, University Press, New York: Oxford (1987).